



**HAL**  
open science

## Rare B decays in BaBar

A. Hicheur

► **To cite this version:**

A. Hicheur. Rare B decays in BaBar. 18th Lake Louise Winter Institute, Feb 2003, Lake Louise Alberta, Canada. pp.248-253. in2p3-00023314

**HAL Id: in2p3-00023314**

**<https://hal.in2p3.fr/in2p3-00023314>**

Submitted on 16 Nov 2004

**HAL** is a multi-disciplinary open access archive for the deposit and dissemination of scientific research documents, whether they are published or not. The documents may come from teaching and research institutions in France or abroad, or from public or private research centers.

L'archive ouverte pluridisciplinaire **HAL**, est destinée au dépôt et à la diffusion de documents scientifiques de niveau recherche, publiés ou non, émanant des établissements d'enseignement et de recherche français ou étrangers, des laboratoires publics ou privés.

## **Rare $B$ decays in BaBar**

A. Hicheur

*On behalf of the BaBar Collaboration*

LAPP-IN2P3-CNRS

9, chemin de Bellevue, BP. 110

F-74941 Annecy-le-Vieux Cedex

Presented at Lake Louise Winter Institute “Particles and the Universe”  
Alberta (Canada), February 16-22, 2003

# RARE $B$ DECAYS IN BABAR

A.HICHEUR

*On Behalf of the BaBar collaboration*

LAPP IN2P3-CNRS

9 Chemin de Bellevue - BP 110

74941 Annecy-le-Vieux CEDEX - FRANCE

E-mail: [hicheur@lapp.in2p3.fr](mailto:hicheur@lapp.in2p3.fr)

Measurements and searches for rare  $B$  decays have been performed with the BaBar detector at the PEP-II  $e^+e^-$  asymmetric  $B$  Factory, operating at the  $\Upsilon(4S)$  resonance. We report some recent branching fraction measurements on hadronic and radiative  $B$  decays, occurring from  $b \rightarrow s/d$  and  $b \rightarrow u$  transitions. Most of the results presented here are based on a data sample corresponding to a luminosity of  $81.9 \text{ fb}^{-1}$ .

## 1. Motivations

Most of the decays of the  $B$  meson occur from a  $b \rightarrow c$  tree transition. This produces final states such as  $B \rightarrow D\pi$ ,  $B \rightarrow D\rho, \dots$

All the decays that don't belong to this category are referred to as rare decays. These are generated by the  $b \rightarrow u$  and the  $b \rightarrow s/d$  loop ("penguin"<sup>1,2</sup>) transitions.

Given the huge data sample available at the  $B$  factories, precise measurements of rare  $B$  decays could be used to probe new physics. This is particularly true for the penguin diagrams where virtual Higgs bosons or SUSY particles could be involved in the loop. On the other hand rare  $CP$  eigenstates bring additional information to test the CKM unitarity triangle.

Direct  $CP$  (or charge) asymmetry defined as:

$$A_{CP} = \frac{\Gamma(\bar{B} \rightarrow \bar{f}) - \Gamma(B \rightarrow f)}{\Gamma(\bar{B} \rightarrow \bar{f}) + \Gamma(B \rightarrow f)} \quad (1)$$

is non-zero only if there are at least two contributing diagrams to a given process, with both different weak and strong phases. It is therefore sensitive to extra contributions arising from new physics for processes driven by a single contribution in the Standard Model.

## 2. Radiative and electroweak penguins

### 2.1. $b \rightarrow s\gamma$

The  $b \rightarrow s\gamma$  transition leads to the decay  $B \rightarrow X_s\gamma$  where  $X_s$  is a strange hadronic system recoiling against an energetic photon.

Two approaches have been adopted: a fully inclusive analysis<sup>3</sup> where only the photon is reconstructed (method *a*) and a semi-exclusive analysis<sup>4</sup> (method *b*) in which a photon, a kaon and up to three pions are combined to form a  $B$  candidate. In both methods, we look for a photon whose energy in the  $\Upsilon(4S)$  center of mass frame ( $E_\gamma^*$ ) is above 2.1  $GeV$  and below 2.7  $GeV$ . Figure 1 shows the resulting  $E_\gamma^*$  spectrum from method *a* and the branching ratio as a function of the  $X_s$  system invariant mass from method *b*, respectively.

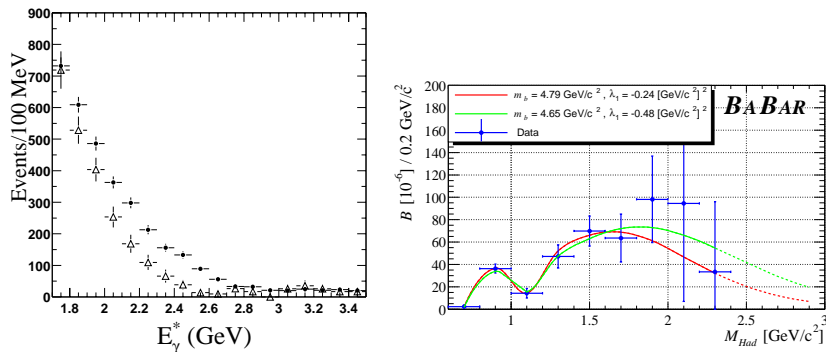


Figure 1.  $B \rightarrow X_s\gamma$  analyses: inclusive photon energy spectrum (data in solid points, background expectation in open triangles) and branching ratio vs.  $m(X_s)$ . The curves superimposed on the  $m(X_s)$  spectrum represent fits relying on heavy quark effective theory parameters.

A fit to the  $m(X_s)$  spectrum enables to extract heavy quark effective theory parameters<sup>5,6</sup>.

The total branching ratio is:

$$\mathcal{B}(B \rightarrow X_s\gamma) = (3.86 \pm 0.36(stat.) \pm 0.37(syst.)_{-0.23}^{+0.43}(model)) \times 10^{-4}$$

for the inclusive analysis and

$$\mathcal{B}(B \rightarrow X_s\gamma) = (4.3 \pm 0.5(stat.) \pm 0.8(syst.) \pm 1.3(model)) \times 10^{-4}$$

for the semi-exclusive analysis.

## 2.2. $B \rightarrow K^{(*)}l^+l^-$

The search for the electroweak penguin transition  $b \rightarrow s l^+l^-$  have been done through the reconstruction of the modes  $B \rightarrow K^{(*)}l^+l^-$ . A charged or neutral  $K$  or  $K^*$  is combined to a  $e^+e^-$  or  $\mu^+\mu^-$  pair to form a  $B$  candidate. Background from the charmonium modes  $B \rightarrow J/\psi K^{(*)}$ ,  $\psi(2S)K^{(*)}$  is vetoed by applying a cut on the lepton pair invariant mass. Figure 2 shows the distribution of beam energy constrained  $B$  mass,  $M_{ES} = \sqrt{E_{beam}^2 - p_B^{*2}}$ , and energy difference,  $\Delta E = E_{beam} - E_B^*$ , for the  $Kl^+l^-$  and  $K^*l^+l^-$  modes.

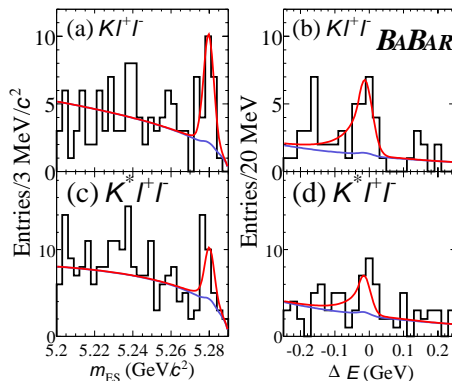


Figure 2.  $M_{ES}$  and  $\Delta E$  projections for the combined  $K l^+l^-$  (a,b) and  $K^* l^+l^-$  (c,d) modes.

The corresponding rates are:

$$\begin{aligned} \mathcal{B}(B \rightarrow K l^+l^-) &= (0.78_{-0.20}^{+0.24}(stat.)_{-0.18}^{+0.11}(syst.)) \times 10^{-6} \\ \mathcal{B}(B \rightarrow K^* l^+l^-) &= (1.68_{-0.58}^{+0.68}(stat.) \pm 0.28(syst.)) \times 10^{-6} \text{ or} \\ &< 3 \times 10^{-6} \text{ @ } 90\% \text{ C.L} \end{aligned}$$

These results are in the range expected in the Standard Model <sup>8,9,10</sup>.

### 3. Hadronic rare decays

Rare hadronic decays<sup>a</sup> can be separated into two categories: those who are dominated by the penguin  $b \rightarrow s/d g^*$  transition and those who are dominated by the suppressed  $b \rightarrow u$  tree transition.

#### 3.1. Gluonic penguins

The decay  $B \rightarrow \eta' K$  is dominated by the  $b \rightarrow sg^*$  transition while  $B \rightarrow \phi K^{(*)}$  is a pure penguin.

The large rate observed for  $B \rightarrow \eta' K$  has stimulated a huge amount of theoretical studies<sup>12,13</sup>. The neutral mode  $B^0 \rightarrow \eta' K_s^0$  is a  $CP$  eigen mode and can be used for the extraction of  $\sin(2\beta)$ .

The  $\eta'$  has been reconstructed in both  $\eta\pi^+\pi^-$  and  $\rho^0\gamma$  channels<sup>14</sup>. Figure 3 shows the  $M_{ES}$  and  $\Delta E$  distributions for  $B^\pm \rightarrow \eta' K^\pm$  and  $B^0 \rightarrow \eta' K_s^0$  channels.

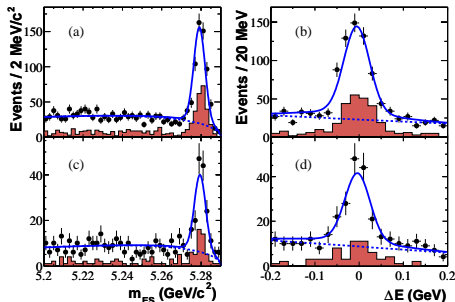


Figure 3.  $M_{ES}$  and  $\Delta E$  projections for  $B^\pm \rightarrow \eta' K^\pm$  (a,b) and  $B^0 \rightarrow \eta' K_s^0$  (c,d). Points with errors represent data, solid curves the full fit functions, and dashed curves the background functions; the shaded histogram represents the  $\eta'_{\eta\pi\pi} K$  subset.

The measured rates are:

$$\begin{aligned} \mathcal{B}(B^\pm \rightarrow \eta' K^\pm) &= (76.9 \pm 3.5(stat.) \pm 4.4(syst.)) \times 10^{-6} \\ \mathcal{B}(B^0 \rightarrow \eta' K_s^0) &= (55.4 \pm 5.2(stat.) \pm 4.0(syst.)) \times 10^{-6} \end{aligned}$$

and the measured charge asymmetry for  $B^\pm \rightarrow \eta' K^\pm$ ,

$$\mathcal{A}_{CP}(\eta' K^\pm) = 0.037 \pm 0.045(stat.) \pm 0.011(syst.),$$

<sup>a</sup>In this note, we only present results on two body modes. Recent measurements of three body charmless decays are detailed in reference<sup>11</sup>

is consistent with zero.

$B \rightarrow \phi K^*$  has been studied in both the charged and neutral modes<sup>15</sup> with  $K^{*\pm}$  being reconstructed in the channels  $K_S^0 \pi^\pm$  and  $K^\pm \pi^0$  and  $K^{*0}$  being reconstructed in the channels  $K^\pm \pi^\mp$  and  $K_S^0 \pi^0$ . Figure 4 shows the  $M_{ES}$  distribution for  $B^\pm \rightarrow \phi K^{*\pm}$  and  $B^0 \rightarrow \phi K^{*0}$ .

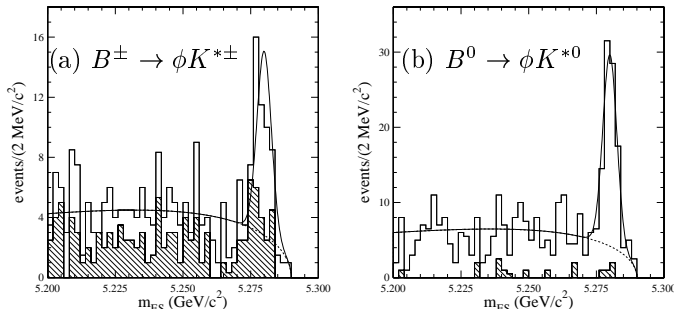


Figure 4.  $M_{ES}$  projections for  $B \rightarrow \phi K^*$ . Open histograms represent the full data, solid curves the full fit functions, and dashed curves the background functions; the hatched histograms represent the  $\phi K^{*\pm} (\rightarrow K^\pm \pi^0)$  and  $\phi K^{*0} (\rightarrow K_S^0 \pi^0)$  subsets.

The branching ratios and charged asymmetries are:

$$\begin{aligned} \mathcal{B}(B^\pm \rightarrow \phi K^{*\pm}) &= (12.1_{-1.9}^{+2.1}(\text{stat.}) \pm 1.5(\text{syst.})) \times 10^{-6} \\ \mathcal{A}_{CP}(\phi K^{*\pm}) &= 0.16 \pm 0.17(\text{stat.}) \pm 0.04(\text{syst.}) \\ \mathcal{B}(B^0 \rightarrow \phi K^{*0}) &= (11.1_{-1.2}^{+1.3}(\text{stat.}) \pm 1.1(\text{syst.})) \times 10^{-6} \\ \mathcal{A}_{CP}(\phi K^{*0}) &= 0.04 \pm 0.012(\text{stat.}) \pm 0.02(\text{syst.}) \end{aligned}$$

### 3.2. Suppressed tree transition

The decay  $B^0 \rightarrow \pi^+ \pi^-$ , dominated by the tree  $b \rightarrow u$  transition, is used for the extraction of  $\sin(2\alpha)$ . For this purpose, one needs to unfold the penguin  $b \rightarrow dg^*$  contribution. This could be done with an isospin analysis involving the measurements of the modes  $B^0 \rightarrow \pi^0 \pi^0$  and  $B^\pm \rightarrow \pi^\pm \pi^0$ <sup>16</sup>. Figure 5 shows the  $M_{ES}$  and  $\Delta E$  distributions for  $B^\pm \rightarrow \pi^\pm \pi^0$ .

A  $B^\pm \rightarrow \pi^\pm \pi^0$  signal is observed with a  $7.7 \sigma$  significance and a charge asymmetry consistent with zero while only a 90% confidence level upper limit on  $B^0 \rightarrow \pi^0 \pi^0$  is set:

$$\begin{aligned} \mathcal{B}(B^\pm \rightarrow \pi^\pm \pi^0) &= (5.5_{-0.9}^{+1.0}(\text{stat.}) \pm 0.6(\text{syst.})) \times 10^{-6} \\ \mathcal{A}_{CP}(\pi^\pm \pi^0) &= -0.03_{-0.17}^{+0.18}(\text{stat.}) \pm 0.02(\text{syst.}) \\ \mathcal{B}(B^0 \rightarrow \pi^0 \pi^0) &< 3.6 \times 10^{-6} \end{aligned}$$

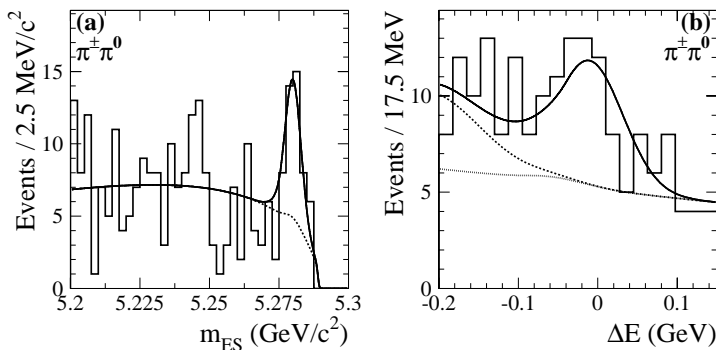


Figure 5.  $M_{ES}$  (a) and  $\Delta E$  (b) projections for  $B^\pm \rightarrow \pi^\pm \pi^0$ . Histograms represent data, solid curves the full fit functions, and dashed curves the background functions.

## References

1. J.Ellis *et al.*, *Nucl. Phys. B* **131**, 285-307 (1977).
2. K.Lingel *et al.*, *Ann. Rev. Nucl. Part. Sci.* **48**, 253 (1998) - hep-ex/9804015.
3. The BaBar collaboration, B.Aubert *et al.*, hep-ex/0207076, submitted to the 31<sup>st</sup> International Conference on High Energy Physics, July 2002 (ICHEP 2002), Amsterdam, The Netherlands.
4. The BaBar collaboration, B.Aubert *et al.*, hep-ex/0207074, submitted to ICHEP 2002, Amsterdam, The Netherlands.
5. A.Kagan and M.Neubert, *Eur. Phys. J.* **C7**, 5 (1999)
6. Z.Ligeti *et al.*, *Phys. Rev. D* **60**, 034019 (1999).
7. The BaBar collaboration, B.Aubert *et al.*, hep-ex/0207082, submitted to ICHEP 2002, Amsterdam, The Netherlands.
8. A.Ali *et al.*, *Phys. Rev. D* **61**, 074024 (2000).
9. A.Faessler *et al.*, *Eur. Phys. J.* **C4**, 18 (2002).
10. M.Zhong *et al.*, hep-ph/0206013, to appear in the proceedings of ESO - CERN - ESA Symposium on Astronomy, Cosmology and Fundamental Physics, Garching, Germany, 4-7 March 2002.
11. The BaBar collaboration, B.Aubert *et al.*, hep-ex/0304006, submitted to *Phys. Rev. Lett.*
12. C-W. Chiang and J.L. Rosner, *Phys. Rev. D* **65**, 074035 (2002), and references therein.
13. M. Beneke and M. Neubert, *Nucl. Phys. B* **651**, 225 (2003).
14. The BaBar collaboration, B.Aubert *et al.*, hep-ex/0303046, submitted to *Phys. Rev. Lett.*
15. The BaBar collaboration, B.Aubert *et al.*, hep-ex/0303020.
16. The BaBar collaboration, B.Aubert *et al.*, hep-ex/0303028, submitted to *Phys. Rev. Lett.*